HIV-1 Nef interferes with T-lymphocyte circulation through confined environments in vivo

Bettina Stolp[a,b], Andrea Imle[a,1], Fernanda Matos Coelho[b,1], Miroslav Hons[b], Roser Gorina[b], Ruth Lyck[b], Jens V. Stein[b,2], and Oliver T. Fackler[a,2]

[a]Department of Infectious Diseases–Virology, University Hospital Heidelberg, 69120 Heidelberg, Germany; and [b]Theodor Kocher Institute, University of Bern, 3012 Bern, Switzerland

Edited by Ronald N. Germain, National Institutes of Health, Bethesda, MD, and accepted by the Editorial Board October 1, 2012 (received for review March 14, 2012)

HIV-1 negative factor (Nef) elevates virus replication and contributes to immune evasion in vivo. As one of its established in vitro activities, Nef interferes with T-lymphocyte chemotaxis by reducing host cell actin dynamics. To explore Nef's influence on in vivo recirculation of T lymphocytes, we assessed lymph-node homing of Nef-expressing primary murine lymphocytes and found a drastic impairment in homing to peripheral lymph nodes. Intravital imaging and 3D immunofluorescence reconstruction of lymph nodes revealed that Nef potently impaired T-lymphocyte extravasation through high endothelial venules and reduced subsequent parenchymal motility. Ex vivo analyses of transendothelial migration revealed that Nef disrupted T-lymphocyte polarization and interfered with diapedesis and migration in the narrow subendothelial space. Consistently, Nef specifically affected T-lymphocyte motility modes used in dense environments that pose high physical barriers to migration. Mechanistically, inhibition of lymph node homing, subendothelial migration and cell polarization, but not diapedesis, depended on Nef's ability to inhibit host cell actin remodeling. Nef-mediated interference with in vivo recirculation of T lymphocytes may compromise T-cell help and thus represents an important mechanism for its function as a HIV pathogenicity factor.

T-lymphocyte homing | two photon intravital microscopy

The Nef protein of HIV and simian immunodeficiency viruses promotes viral replication in vivo and rapid progression to AIDS. Numerous in vitro functions mediated by specific protein–protein interactions were assigned to Nef by which the viral protein affects host cell intracellular transport and signal transduction (1). How these functions individually contribute to the prominent role of Nef in AIDS pathogenesis remains to be established. Inhibition of dynamic host cell actin remodeling, mediated via association with the cellular kinase PAK2 that induces inactivation of the actin-severing factor cofilin to reduce actin turnover, represents a conserved activity of lentiviral Nef proteins (2–8). Nef-PAK2 association depends on a critical phenylalanine at position 195 of Nef (or 191 depending on the HIV-1 *nef* allele analyzed) that is dispensable for other Nef activities (9). Disruption of host cell actin remodeling by Nef does not affect intrinsic replication properties of HIV-1 (10, 11) but Nef impairs T-lymphocyte chemotaxis in vitro (12–14). Whether Nef also affects T-lymphocyte motility in mammals, which is only in part driven by chemokines (15), has not yet been addressed.

Physiologically, T lymphocytes continuously traffic between blood and secondary lymphoid organs. For entry into lymph nodes, T lymphocytes use CD62L to transiently attach to high endothelial venules (HEV) that pass through the T-cell areas of lymph nodes. Subsequently, T lymphocytes are activated by the surface-bound chemokine CCL-21, which through its receptor CCR7 triggers lymphocyte function-associated antigen 1-dependent shear-resistant firm arrest. Before diapedesis, T lymphocytes acquire a polarized cell shape and actively migrate on the luminal surface of HEVs, presumably to find an appropriate egress site (16). After diapedesis, lymphocytes remain attached for a few minutes in the perivascular space before being finally released into the underlying parenchyma (16, 17). The subendothelial migration away from transmigration sites into the underlying tissue represents the last critical step and allows actual entry of T lymphocytes into the T-cell area of lymphoid organs (16, 18). Within the T-cell area, T lymphocytes crawl with an average speed of 15 μm/min along the 3D network of fibroblastic reticular cells and screen antigen-presenting cells for antigens. Notably, HEVs are tightly surrounded by matrix but the lymph-node parenchyma is less tightly packed with fibers as migration tracks, indicating that T lymphocytes face microenvironments with different densities during these migration steps (19). In the absence of cognate antigens, T lymphocytes exit lymph nodes within 12–24 h. Repetitive homing to and egress from lymph nodes thus requires active migration of T lymphocytes and represents a prerequisite for proper immune surveillance and screening of rare antigen-specific T lymphocytes for cognate antigen (18).

In this study we use a combination of in vivo and ex vivo model systems to quantify and visualize the effects of HIV-1 Nef on physiological circulation of T lymphocytes.

Results

HIV-1 Nef Is Functional Following Retroviral Transduction and Isolation of Primary Murine T Lymphocytes. To investigate whether the inhibition of T-lymphocyte motility observed in vitro is relevant for Nef's role in HIV pathogenesis, we established an experimental strategy that mimics aspects of acute HIV-1 infection by expression of Nef in murine T lymphocytes for subsequent adoptive transfer and functional characterization of their homing behavior (Fig. S1). Expressed upon optimized transduction with murine leukemia virus vectors (20), Nef.GFP displayed full biological activity in primary mouse T lymphocytes, including cell-surface receptor down-modulation, inhibition of chemokine-induced actin remodeling (2), induction of high levels of phosphorylated (inactive) cofilin (5), targeting of Lck kinase to intracellular membrane compartments (21), and chemotaxis through 3- and 5-μm transwell membranes (22) (Fig. S2). Similar to human cells (5), the PAK2-association deficient Nef mutant F195A did not interfere with actin remodeling and host cell motility in transduced primary murine T lymphocytes. Similar results were obtained following magnetic bead selection of (>95% $NGFR^+$) primary mouse T lymphocytes transduced with *IRESΔngfr* versions of these expression constructs encoding for NGFR with cytoplasmic tail deletion and nonfusion Nef. Nef

Author contributions: B.S., J.V.S., and O.T.F. designed research; B.S., A.I., F.M.C., M.H., and R.G. performed research; R.G. and R.L. contributed new reagents/analytic tools; B.S., A.I., F.M.C., J.V.S., and O.T.F. analyzed data; and J.V.S., B.S., and O.T.F. wrote the paper.

The authors declare no conflict of interest.

This article is a PNAS Direct Submission. R.N.G. is a guest editor invited by the Editorial Board.

[1]A.I. and F.M.C. contributed equally to this work.

[2]To whom correspondence may be addressed. E-mail: jens.stein@tki.unibe.ch or oliver.fackler@med.uni-heidelberg.de.

This article contains supporting information online at www.pnas.org/lookup/suppl/doi:10.1073/pnas.1204322109/-/DCSupplemental.

expression levels were identical to those in HIV-1 infected human T lymphocytes (Fig. S3). Our transduction/isolation strategy thus allows for functional analysis of homogenously Nef-expressing primary mouse T lymphocytes in which Nef exerts its activities in analogy to HIV-1 infection of primary human T lymphocytes.

HIV-1 Nef Efficiently Interferes with T-Lymphocyte Homing to Lymph Nodes. Next, transduced and sorted cell populations were labeled with CellTracker dyes ex vivo for subsequent detection and adoptively transferred into recipient mice to assess whether expression of WT or F195A Nef influences T-lymphocyte trafficking in vivo. Four and 24 h posttransfer, spleen, and peripheral (pLN) and mesenteric (mLN) lymph nodes were harvested and analyzed independently for homing efficiency of adoptively transferred cells by flow cytometry. As an internal homing control, cells expressing the empty vector were cotransferred together with equal amounts of WT or F195A Nef-expressing cells. Nef expression only slightly affected homing to spleen (Fig. 1*A*) (31 ± 31% and 34 ± 23% reduced homing compared with control at 4 h and 24 h, respectively), a process that does not require the crossing of an endothelial barrier (18). In contrast, Nef caused a marked reduction of T-lymphocyte homing to the pLN (Fig. 1*B*) and mLN (Fig. 1*C*). This inhibition was observed at the early 4 h homing time-point (75 ± 13% and 63 ± 20% reduced homing compared with control cells for pLNs and mLNs, respectively) as well as after 24 h when equilibrium between homing and egress is reached (62 ± 6% and 64 ± 5% reduced homing compared with control cells for pLNs and mLNs, respectively). Nef F195A was partially defective in blocking lymph node homing at the 4 h time-point. However, 24 h posttransfer, similar amounts of control and Nef F195A-expressing cells were observed in secondary lymphoid organs. Because our transduction strategy did not distinguish between $CD4^+$ and $CD8^+$ T lymphocytes, and only $CD4^+$ cells are physiological targets of HIV-1 infection, homing of both populations was also assessed separately. Notably, homing of in vitro mitogen-stimulated $CD8^+$ T lymphocytes was about fourfold less efficient compared with homing of $CD4^+$ T lymphocytes, and homing to spleen and lymph nodes of $CD4^+$ T lymphocyte was more potently blocked by Nef than that of $CD8^+$ T lymphocytes (Fig. S4). In contrast to the situation in $CD4^+$ T lymphocytes, the moderate effects of Nef on homing of $CD8^+$ T lymphocytes did not depend on the F195 motif. HIV-1 Nef thus efficiently interferes with homeostatic trafficking of $CD4^+$ T lymphocytes in vivo.

HIV-1 Nef Interferes with T-Lymphocyte Transmigration Under Shear. We next asked at which specific step Nef interferes with T lymphocyte trafficking during the homing process. Because transmigration across the endothelial cells lining HEVs constitutes a critical step in the homing process, we first addressed whether Nef affects crawling and diapedesis through an endothelial cell monolayer under shear flow (23, 24). Transduced and purified T lymphocytes were differentially labeled with CellTracker dyes in vitro, mixed, and perfused over a CCL-21–coated primary brain microvascular endothelial cell monolayer to image the recruitment process by video microscopy over 50 min (Fig. 2*A* and Movie S1). Frame-by-frame offline analysis of transendothelial migration (TEM) under shear flow enabled us to dissect which step of the TEM process is influenced by Nef. T lymphocytes were allowed to accumulate on the endothelium at low shear stress (0.15 dyn/cm^2) and after the accumulation phase flow was increased to physiological shear stress (1.5 dyn/cm^2). TEM is initiated by capture of the T lymphocytes to the endothelium during the accumulation phase, followed by the acquisition of a polarized phenotype and an optional crawling step to find permissive sites for diapedesis (24). In contrast to previous studies that addressed effects of Nef on cell adhesion in the absence of physiological shear flow (8, 14), WT or F195A Nef did not affect the initial accumulation of T cells on the CCL-21–coated endothelium under our shear-flow conditions (Fig. 2*B*). Most control cells acquired a polarized shape after binding to the endothelial cell layer (Fig. 2*C*). In contrast, Nef-expressing T cells were significantly less elongated at all time-points analyzed than were control cells. Defects in cell polarization were also observed in the absence of shear flow upon plating of transduced and purified T lymphocytes on fibronectin-coated surfaces and stimulation with CCL-21 to analyze efficient formation of a leading and trailing edge. This disruption of cell polarization by Nef in the absence or presence of shear flow was strictly dependent on its F195 motif (Fig. 2 *C* and *D*, and Fig. S5 *A* and *B*), indicating that functional actin remodeling is crucial for proper cell polarization after adhesion.

To assess whether locomotion of T lymphocytes on the endothelium subsequent to firm arrest is affected by Nef, single cells were manually tracked until they successfully transmigrated (Fig. 2*A*, cell marked with the orange arrowhead at 900 s). After adhesion, control T lymphocytes immediately started to transmigrate and only few additional diapedesis events were observed after the first 20 min of observation (Fig. 3*B*). Because most cells transmigrated nearby the site of their first attachment to the endothelium and thus underwent minimal lateral locomotion before transmigration, Nef only marginally affected lateral locomotion distance and velocity of T lymphocytes before diapedesis (Fig. S6) and consistently did not exert major effects on the activity of the Rac1 GTPase that is required for these early events (Fig. S5*C*) (23, 24). In contrast, Nef-expressing cells showed significantly less diapedesis events and transmigrated with delayed kinetic relative to control cells (Fig. 3 *A* and *B*). Quantification of transmigration efficiency revealed a twofold block in diapedesis imposed by Nef (Fig. 3*A*, "diapedesis") (71 ± 14 vs. 35 ± 8%). Cells that were not transmigrating remained adhered on the surface of the endothelium during the entire observation period (Fig. 3*A*, "on top"). Importantly, diapedesis of Nef F195A-expressing cells was equally impaired to that of WT Nef expressing cells and Nef did not disrupt formation of potentially invasive and chemokine-sensing filopodia (25) (Fig. S7). Thus, HIV-1 Nef potently blocks lymphocyte diapedesis via a mechanism that does not involve its ability to interfere with actin remodeling.

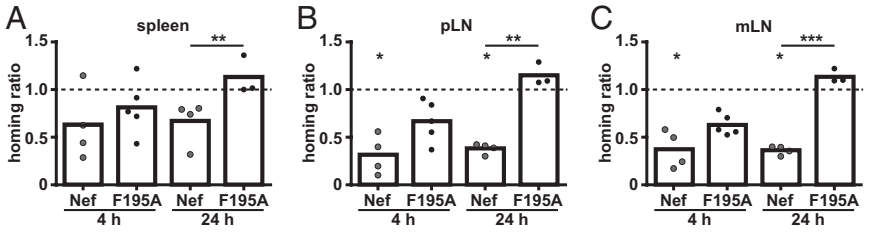

Fig. 1. Nef interferes with T-lymphocyte homing to lymph nodes. Primary T lymphocytes were isolated, transduced, and sorted (Fig. S3), labeled with CellTracker dyes, and adoptively transferred into recipient mice. Control cells were always coinjected with Nef WT or F195A-expressing T lymphocytes as an internal control. Spleen (*A*), pLN (*B*), and mLN (*C*) were harvested after 4 or 24 h and single-cell suspensions were analyzed by flow cytometry. The homing ratio in each mouse was calculated relative to coinjected control cells, arbitrarily set to 1 (indicated by the dashed line). Each circle represents data from one animal. *P* values were calculated performing a Kruskal–Wallis test with a Dunn's posttest. **P* < 0.05; ***P* < 0.005; ****P* < 0.0005.

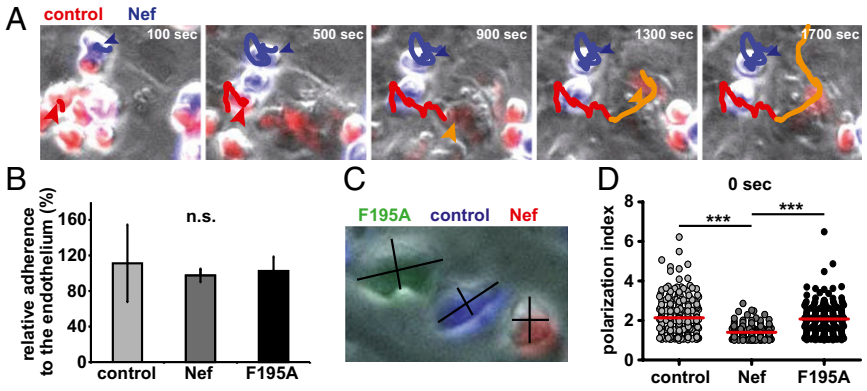

Fig. 2. Nef interferes with transendothelial migration and polarization of T lymphocytes on the endothelium. Twenty-four hours posttransduction and sorting, primary T lymphocytes were labeled with one of three different CellTracker dyes (CMTMR/red, CMAC/blue, CFSE/green), mixed in equal amounts and applied to a TNF-α–stimulated, CCL-21–coated primary murine brain endothelium under low shear flow (0.15 dyne/cm^2). After efficient cell attachment had occurred (about 60 s), shear flow was increased (1.5 dyne/cm^2), and TEM was monitored over 50 min with one image acquired every 20 s. (*A*) Still images of Movie S1 showing a representative field-of-view of a TEM experiment. Shown is an endothelial cell monolayer with control and Nef expressing T lymphocytes, labeled in red and blue, respectively. Colored lines highlight migration tracks of one Nef-expressing cell (blue line) and one control cell (red line, orange following diapedesis). The Nef-expressing cell is additionally highlighted by a blue arrowhead, one representative control cell is marked by a red arrowhead, which turns orange following diapedesis. (*B*) Relative efficiency of adherence to the endothelium under shear flow. Shown is the percentage of input cells that attached to the endothelial cell monolayer at the time-point when higher shear flow rates are first applied (60 s of imaging). (*C*) Polarization indices were calculated by dividing cell length by cell width at three different time points, One is shown here. (*D*) Polarization indices of single cells directly after (0 s) increasing shear flow from three independent TEM experiments, measured as shown in *C*. Red bars indicate mean values. *P* values were calculated using a one-tailed ANOVA test with a Newman–Keuls posttest. n.s., not significant. Images were acquired using a 20 × objective. ***$P < 0.0005$.

Nef Impairs Subendothelial Migration. Following successful diapedesis, T lymphocytes proceed to crawl underneath the endothelium as an important step for dissemination into the target tissue (16, 18, 26). We therefore tracked subendothelial T lymphocyte motility after diapedesis (Figs. 2*A*, orange part of the track, 3*C*, and Movie S2). Although control lymphocytes displayed long migration paths in this highly confined microenvironment, most Nef-expressing cells were unable to move away from their initial site of diapedesis. As a result, these cells covered significantly shorter migration distances and migrated with reduced velocities (Fig. 3*D*) (42% of the velocity of control cells). Similar to in vitro chemotaxis (Figs. S2 *E* and *F* and S3*E*) and lymph node homing at early time-points (Fig. 1 *B* and *C*), this effect largely depended on the F195 PAK2-association motif (Fig. 3 *C* and *D*). Inhibition of subendothelial T-lymphocyte migration by Nef following diapedesis thus likely involves inhibition of actin remodeling. With diapedesis and subsequent subendothelial migration, Nef inhibits two distinct and essential steps for T-lymphocyte TEM by genetically separable mechanisms.

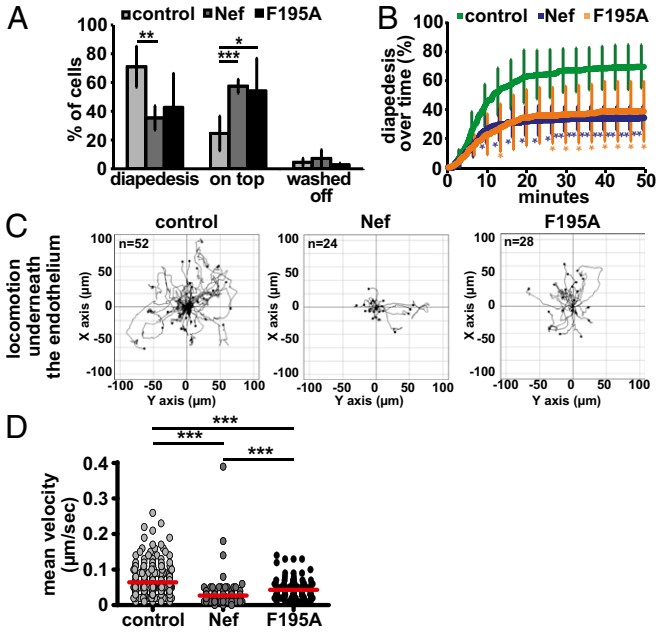

Fig. 3. Nef-expression interferes with T-lymphocyte subendothelial motility. TEM assays of transduced/sorted T lymphocytes as in Fig. 2. (*A*) Quantification of the percentage of cells that perform diapedesis, remain on top of the endothelium (on top) or are washed off the endothelium by the shear flow (washed off). Shown are mean values of four to five independent experiments with SD. *P* values were calculated performing a Student *t* test. (*B*) Kinetics of diapedesis during the 50-min time course of imaging. Shown are mean values from four independent experiments with SD. *P* values relative to the control were calculated performing a Student *t* test. (*C*) Tracks of single cells crawling underneath the endothelium derived from one of four to five representative TEM experiments. T lymphocytes were tracked manually after successful diapedesis. (*D*) Mean velocity of single cells migrating underneath the endothelial cell monolayer, calculated from single-cell tracks, as shown in *C* from four to five independent TEM experiments. Red bars indicate mean values. *P* values were calculated using a one-tailed ANOVA test with a Newman–Keuls posttest. *$P < 0.05$; **$P < 0.005$; ***$P < 0.0005$.

Nef Interferes with T-Lymphocyte Motility in Confined 3D Matrices. The above results revealed that Nef specifically affects diapedesis and subendothelial migration. Reflecting the need for acquiring motility in distinct physiological environments with varying degrees of confinement, leukocytes adopt different motility modes involving distinct machineries in response to select extracellular cues (27). We therefore tested whether the ability of Nef to block T-lymphocyte motility is related to the density and texture of 3D environments, using well-established collagen matrices as models for pore-size restricted migration. Transduced/isolated T lymphocytes were embedded into low-density or high-density collagen matrices in the presence of CCL-21, and migration of control and Nef-expressing cells in these 3D cultures was followed by time-lapse microscopy over a time-course of 2.5 h. In low-density collagen and thus absence of significant physical barriers, shape and length of tracks of Nef-expressing cells, as well as their velocity, were indistinguishable from those of control cells (Fig. 4 *A* and *C*, Fig. S8*A*, and Movie S3). In contrast, the motility of Nef-expressing T lymphocytes was significantly impaired relative to control cells in the more compact environment of a high-density collagen matrix (Fig. 4*B*, Fig. S8*B*, and Movie S4), in which cells require higher contractile force generation for locomotion (27). This finding was reflected in an approximately 35% reduced velocity of Nef-expressing cells in high-density collagen (Fig. 4*D*). This motility inhibition by Nef strictly depended on its ability to interfere with actin remodeling (Fig. 4*D*) (control: 1.8± 0.9 μm/min, Nef: 1.2± 0.9 μm/min; F195A: 1.7 ± 0.8 μm/min). Nef thus specifically inhibits T

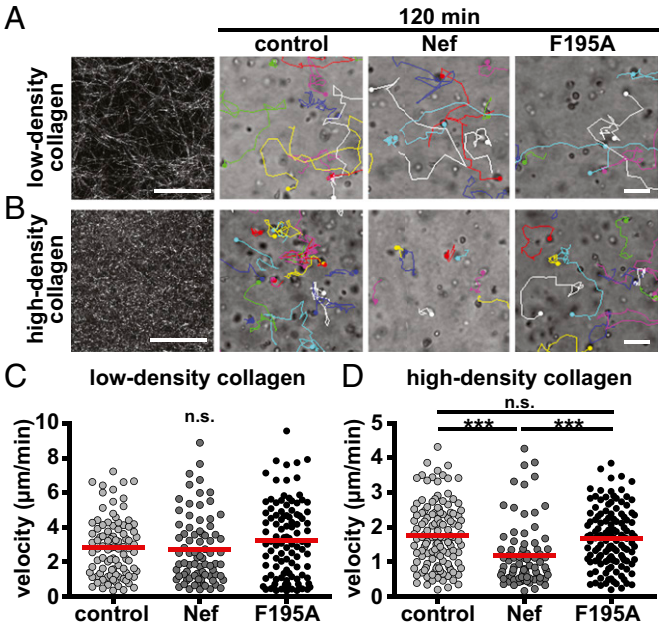

Fig. 4. Nef interferes with T-lymphocyte motility in 3D matrices dependent on the pore size. Transduced/sorted T lymphocytes were embedded into collagen matrices of different densities in the presence of 100 ng/mL CCL-21. Migration of cells was monitored by bright-field microscopy over 2.5 h with one image acquired every 3 min. Shown are still images of a representative field of view of a time-lapse 3D migration experiment at the 120-min time point. (*A*) Low-density collagen (1.6 mg/mL) showing stills of Movie S3. (*B*) High-density collagen (4.6 mg/mL) showing stills of Movie S4. (*Left*) Fibrillar structures of the collagen preparations used visualized as maximum projections of 10-μm stacks using confocal reflection microscopy. Moving cells are labeled with colored dots and their tracks are indicated over time. (Scale bars, 50 μm.) Mean velocities per cell have been calculated from single-cell tracks as shown in *A* and *B* for low- (*C*) and high-density (*D*) collagen matrices. Shown are results from one representative experiment of three. Red bars indicate mean values. *P* values were calculated performing a Mann–Whitney test. n.s., not significant. ***$P < 0.0005$.

lymphocyte motility modes used in high-density environments with high physical constraints, and 3D collagen matrices represent a suitable experimental system for the analysis of this process.

Nef-Expressing Cells Are Retained in HEVs and Show Reduced Motility in pLNs. We next analyzed whether the blocks conferred by Nef to T lymphocyte diapedesis and motility in confined environments in vitro might explain the defect observed in lymph node homing. Transduced/isolated T lymphocytes were labeled with CellTracker dyes, adoptively transferred into recipient mice and allowed to home for 30 min, followed by 3D immunofluorescence (3-DIF) analysis to determine the precise localization of transferred T lymphocytes (28). Two-times more Nef-expressing than control cells were injected to normalize for the homing defect imposed by Nef expression. Our 3D reconstructions revealed that the majority of control cells had moved away from the HEV network to enter the lymph node parenchyma. In contrast, Nef-expressing cells were often detected inside and close to HEVs (Fig. 5*A*). Quantification of intralymph node localization by 3-DIF revealed Nef-expressing cells to be approximately Twofold-enriched over control cells in the intravascular and perivascular space in all three animals analyzed (Fig. 5*B*). In line with our ex vivo analysis, these results indicate that Nef impairs T lymphocyte diapedesis in vivo to reduce extravasation of T lymphocytes from HEVs into lymph nodes.

To assess whether Nef affects the dynamic in vivo motility of T lymphocytes at and inside lymph nodes, we performed two-photon microscopy (2PM)-based intravital imaging of T-lymphocyte migration. The 2PM confirmed that Nef expressing T lymphocytes were enriched inside HEVs and analysis of single cells revealed that these cells migrated slower in and near HEVs relative to control cells (Fig. 5 *C*, *Upper*, and *D*, and Movie S5) (median: 5.1 vs. 8.1 μm/min). Nef-expressing T cells also migrated with slightly reduced instantaneous velocities (velocity between two frames) compared with control cells inside the lymph node parenchyma (Fig. 5 *C*, *Lower*, and *E*, and Movie S6) (median: 11.0 vs. 8.1 μm/min). As a result, the motility coefficient that provides a measure for the ability of a randomly migrating cell to move away from its starting position was reduced about 40% upon Nef expression in HEVs, as well as in the parenchyma, compared with control cells (Fig. 5*F*). Taken together, these results reveal that Nef mediates a marked block in vivo to the diapedesis of T lymphocytes from HEVs into lymph nodes to reduce homing efficiencies, and exerts moderate effects on subsequent parenchymal motility.

Discussion

Based on quantification and visualization by 3-DIF and intravital 2PM techniques, we demonstrate here that HIV-1 Nef interferes with trafficking of $CD4^+$ T lymphocytes in vivo and specifically impairs their homing to lymph nodes at the transmigration step from the HEV into the lymph node parenchyma. This approach revealed a potent Nef-mediated block to T-lymphocyte homing that is predominantly imprinted at the diapedesis step, with Nef causing an additional but less-pronounced reduction in interstitial motility of T lymphocytes that had successfully entered the lymph node parenchyma. The significantly less-potent inhibition of lymph node homing observed with the F195A Nef mutant suggests that this block critically involves Nef-mediated inhibition of actin remodeling via PAK2-dependent cofilin phosphorylation. Additional mechanisms independent of actin remodeling are clearly involved in the decrease of T-lymphocyte homing to lymph nodes and might include the slight reduction of cell-surface exposure of the homing receptors CD62L and CCR7 observed in the presence of WT and F195A Nef proteins (Fig. S2*B*). Because Nef also inhibited T-lymphocyte chemotaxis toward sphingosine-1-phosphate (S1P), a key chemoattractant involved in lymphocyte exit from lymph nodes (Fig. S8*C*), the viral protein may as well affect egress of infected T lymphocytes from lymph nodes. This effect may increase the density of infected cells inside lymph nodes and thus facilitate virus spread by enhancing the probability for virus cell-to-cell transmission.

The use of an ex vivo cell system to analyze the influence of Nef on diapedesis through primary endothelial cells under physiological shear flow by video microscopy allowed us to recapitulate this Nef-mediated block in TEM and to dissect which step is specifically affected by Nef. Somewhat surprisingly, given its ability to disrupt triggered actin remodeling, Nef did not affect early steps of the TEM process, including shear-resistant attachment, crawling on the endothelial surface, and formation of potentially invasive and chemokine-sensing filopodia. Nef thus distinguishes between host cell protrusions to achieve simultaneous inhibition of sheet-like actin-rich protrusions, such as lamellipodia (25) and promotion of filopodia formation (8, 10). Of note, Murooka et al. recently described that HIV-1–infected T cells in lymph nodes of humanized mice display reduced motility and form long filopodia-like cell protrusions or nanotubes that facilitate virus transfer to neighboring cells in a manner dependent on the HIV glycoprotein Env (29). Our results are consistent with these observations and suggest Nef as an additional HIV protein that is directly involved in these phenomena. In this scenario, Nef likely promotes nanotube/filopodia formation via its recently described association with the exocyst complex, an established regulator of nanotube generation (30).

Potentially indicative of high selective pressure on this Nef activity, Nef inhibited two later steps of TEM via independent mechanisms. First, Nef interfered directly with the diapedesis step via a mechanism that did not involve its ability to interfere with

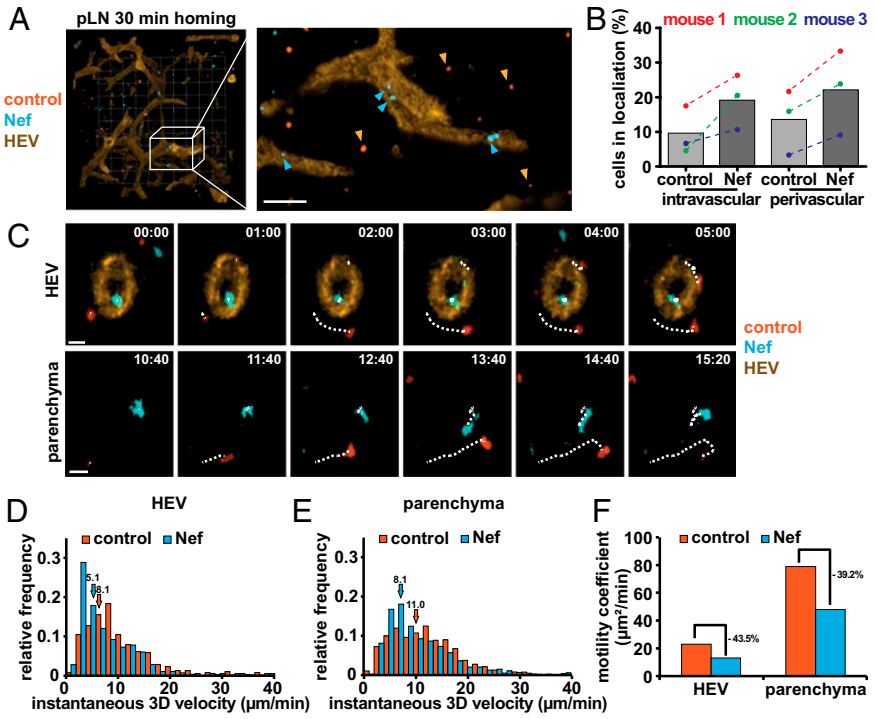

Fig. 5. Nef-expressing cells are retained in HEVs and show reduced motility in pLNs. Primary mouse T lymphocytes were isolated, transduced, and sorted as described in Fig. S3, labeled with CellTracker dyes, and adoptively transferred into recipient mice. Two-times more Nef-expressing T lymphocytes (blue) were coinjected with control cells (red) to normalize for the homing defect imposed by Nef. (*A*) Representative 3-DIF reconstruction of a pLN. Twenty-minutes postadoptive transfer fluorescently labeled MECA-79 was injected intravenously to label HEVs and pLNs were harvested after another 10 min. (Grid, 40 μm.) Magnification shows a maximum projection image of the indicated area. (Scale bar, 40 μm.) Blue and orange arrowheads indicate Nef-expressing and control cells, respectively. (*B*) Quantification of cells localized in HEVs (intravascular), near to HEVs (perivascular), or in the lymph node parenchyma as assessed manually from stacks of 3-DIF images, as shown in *A*. Shown are results from three independent mice (colored individual datapoints) and mean values from all three mice (histogram) with at least 100 cells counted per condition. (*C*) Still images of the 2PM intravital microscopy Movies S5 and S6. Twenty-four hours postadoptive transfer mice were anesthetized and popliteal lymph nodes were surgically exposed to allow intralymph node imaging. (*Upper*) Migration of T lymphocytes in or near HEVs; (*Lower*) migration in the parenchyma. Dotted lines indicate tracks of individual cells. (Scale bars, 10 μm.) Instantaneous 3D velocity of Nef-expressing and control cells as calculated from single cell tracks, as shown in *C*, of cells in or near HEVs (*D*) or the lymph node parenchyma (*E*). Quantifications are derived from intravital microscopy of four independent mice and arrows indicate the median instantaneous velocity of the indicated cell populations. (*F*) Motility coefficients of Nef-expressing and control cells calculated from the data shown in *D* and *E*.

chemokine-induced actin remodeling. Although Nef expression reduced T-cell polarization on CCL-21–coated endothelium, the inhibition of TEM was comparable to F195A-expressing T cells. Polarization is thus not a prerequisite for successful TEM under shear, which reflects previous observations that T lymphocytes undergo TEM despite impaired polarization because of deletion/mutations of Rac or Rac activators (16, 23, 25). Detailed analysis of single cells indicated that protrusions into the subendothelial space are readily observed for Nef-expressing cells, but translocation of the cell body to complete diapedesis was impaired, indicating that Nef does not block diapedesis initiation but completion. These later stages of diapedesis are determined by successive protein–protein interaction steps, involving VE-cadherin, JAM family proteins, and CD99 (31), and depend on the cells' ability to dynamically adapt their overall shape as well as that of their nucleus. Because all these aspects represent potential targets of Nef, deciphering of the exact step and the molecular targets affected by Nef represents an interesting aspect for future research. Second, Nef interfered with motility of T lymphocytes underneath the endothelial cell surface. This effect strictly required the integrity of the F195 motif and thus correlated with Nef's ability to interfere with dynamic actin remodeling. In line with this finding, diapedesis and subendothelial locomotion, but not arrest on the endothelium, strongly depend on F-actin integrity (32), and regulators of F-actin dynamics govern T-lymphocyte crawling or polarization (23, 33–36). Taken together, these findings suggest that the observed polarity defect represents the key consequences of Nef-mediated disruption of actin dynamics, which in turn determines the reduced migratory capacity of Nef-expressing T lymphocytes.

Nef only exerted mild effects on T-lymphocyte crawling on top of the endothelium but almost completely arrested locomotion in the confined subendothelial space. These results were mirrored in 3D matrices where Nef specifically inhibited T-lymphocyte motility in high-density collagen, although motility at low collagen density remained unaffected by Nef expression. It thus emerges that Nef specifically interferes with cell-motility modes that rely on the generation of contractile force to overcome physical constraints of the direct environment, including T-lymphocyte chemotaxis across transwell membranes (4, 5, 12, 14) and diapedesis (present study). This specificity would also explain why Nef-mediated inhibition is relatively moderate on T-lymphocyte homing to spleen, which does not involve the crossing of an endothelial barrier, and motility in the lymph node parenchyma, where lymphocytes are embedded in a relatively wide-spaced extracellular matrix structure (19). In contrast, motility in the confined subendothelial space depends on the formation of sheet-like protrusions (37) that are efficiently targeted by Nef to impair cell motility. Taken together, these data show that the dual mechanism by which Nef interferes with T-lymphocyte TEM likely explains, at least in part, the inhibition of homing to lymph nodes observed in vivo.

T-lymphocyte trafficking and homing is crucial for immune surveillance and rapid eliciting of adaptive immune responses (18). Based on the inhibitory effects of Nef on T-lymphocyte homing and diapedesis, the viral protein would be expected to impair mounting of a specific humoral immune response in HIV-infected patients. Indeed, B-cell dysfunction characterized already at early stages of HIV-1 infection by the lack of high-affinity antibodies is increasingly recognized as a hallmark of AIDS pathogenesis (38, 39). Nef is suggested to contribute to this phenomenon by impairing antigen presentation and prevention of B-cell class switching following transfer from infected cells (40–43). The results presented herein, in line with those from other laboratories (44, 45), suggest that Nef also suppresses B-cell help by HIV-1–infected T lymphocytes. In addition, the observed reduction of parenchymal lymphocyte motility may facilitate cell-associated virus spread in the context of HIV-1 infection. Subversion of host cell motility thus emerges as a cardinal function of Nef likely to play an important role in AIDS pathogenesis.

Materials and Methods

The 3-DIF imaging was essentially performed as described previously (16). Briefly, transduced and NGFR-sorted T lymphocytes were labeled with CellTracker dyes, as described in *SI Materials and Methods*. The 3×10^6 IRESΔNGFR control cells were coinjected with $6–8 \times 10^6$ Nef WT-expressing cells into the retrobulbar sinus of 6- to 8-wk-old WT C57BL/6 mice. Thirty minutes and 24 h after adoptive transfer, pLNs were harvested and fixed overnight in 0.5% paraformaldehyd. Lymph nodes were manually cleaned from surrounding fat, embedded into 1.3% (wt/vol) agarose, dehydrated in methanol for 24 h, and cleared for at least 2 d in benzyl alcohol-benzyl benzoate (1:2 ratio). One-to-two scans were acquired per lymph node using a TrimScope 2PM (LaVisionBiotec) equipped with a Ti:Sapphire laser (MaiTai HP; Spectraphysics) and 20× objective (Olympus) with a scan volume ranging from $0.4 \times 0.4 \times 0.4–0.6$ mm ($0.06–0.1$ mm^3). The absolute number of lymphocytes labeled with each dye was counted using a 3D image analysis software program (Velocity, PerkinElmer). Visual analysis of individual *z*-sections was used to determine the position of individual cells relative to the HEV network.

ACKNOWLEDGMENTS. We thank Reno Debets for the kind gift of the murine leukemia viurs proviral constructs; Nadine Tibroni for expert technical help; Oliver Keppler for help with the organization of the in vivo experiments; and the Scanning Electron Microscopy facility of the microscopy imaging center of the University of Bern for service. This work was supported by the Deutsche Forschungsgemeinschaft SFB638, Project A11 and Grant FA 378/10-1 (to O.T.F) and Fellowship GRK1188 (to B.S.); Swiss National Foundation Grants SNF_135649 (to J.V.S.) and SNF 31003A_133092 (to Britta Engelhardt and R.L.); a Marie Curie postdoctoral fellowship (to F.M.C.); a Leopoldina/Nationale Akademie der Wissenschaften fellowship (to B.S.); and a Swiss Multiple Sclerosis Society grant (to R.L.). R.G. was funded by the Olga Mayenfisch Foundation (to Britta Engelhardt).

1. Laguette N, Brégnard C, Benichou S, Basmaciogullari S (2010) Human immunodeficiency virus (HIV) type-1, HIV-2 and simian immunodeficiency virus Nef proteins. *Mol Aspects Med* 31(5):418–433.
2. Haller C, et al. (2006) The HIV-1 pathogenicity factor Nef interferes with maturation of stimulatory T-lymphocyte contacts by modulation of N-Wasp activity. *J Biol Chem* 281(28):19618–19630.
3. Rudolph JM, Eickel N, Haller C, Schindler M, Fackler OT (2009) Inhibition of T-cell receptor-induced actin remodeling and relocalization of Lck are evolutionarily conserved activities of lentiviral Nef proteins. *J Virol* 83(22):11528–11539.
4. Stolp B, Abraham L, Rudolph JM, Fackler OT (2010) Lentiviral Nef proteins utilize PAK2-mediated deregulation of cofilin as a general strategy to interfere with actin remodeling. *J Virol* 84(8):3935–3948.
5. Stolp B, et al. (2009) HIV-1 Nef interferes with host cell motility by deregulation of Cofilin. *Cell Host Microbe* 6(2):174–186.
6. Fackler OT, Luo W, Geyer M, Alberts AS, Peterlin BM (1999) Activation of Vav by Nef induces cytoskeletal rearrangements and downstream effector functions. *Mol Cell* 3 (6):729–739.
7. Lu TC, et al. (2008) HIV-1 Nef disrupts the podocyte actin cytoskeleton by interacting with diaphanous interacting protein. *J Biol Chem* 283(13):8173–8182.
8. Nobile C, et al. (2010) HIV-1 Nef inhibits ruffles, induces filopodia, and modulates migration of infected lymphocytes. *J Virol* 84(5):2282–2293.
9. Agopian K, Wei BL, Garcia JV, Gabuzda D (2006) A hydrophobic binding surface on the human immunodeficiency virus type 1 Nef core is critical for association with p21-activated kinase 2. *J Virol* 80(6):3050–3061.
10. Haller C, Tibroni N, Rudolph JM, Grosse R, Fackler OT (2011) Nef does not inhibit F-actin remodelling and HIV-1 cell-cell transmission at the T lymphocyte virological synapse. *Eur J Cell Biol* 90(11):913–921.
11. Schindler M, et al. (2007) Association of Nef with p21-activated kinase 2 is dispensable for efficient human immunodeficiency virus type 1 replication and cytopathicity in ex vivo-infected human lymphoid tissue. *J Virol* 81(23):13005–13014.
12. Choe EY, Schoenberger ES, Groopman JE, Park IW (2002) HIV Nef inhibits T cell migration. *J Biol Chem* 277(48):46079–46084.
13. Janardhan A, Swigut T, Hill B, Myers MP, Skowronski J (2004) HIV-1 Nef binds the DOCK2-ELMO1 complex to activate rac and inhibit lymphocyte chemotaxis. *PLoS Biol* 2(1):E6.
14. Park IW, He JJ (2009) HIV-1 Nef-mediated inhibition of T cell migration and its molecular determinants. *J Leukoc Biol* 86(5):1171–1178.
15. Worbs T, Mempel TR, Bölter J, von Andrian UH, Förster R (2007) CCR7 ligands stimulate the intranodal motility of T lymphocytes in vivo. *J Exp Med* 204(3):489–495.
16. Boscacci RT, et al. (2010) Comprehensive analysis of lymph node stroma-expressed Ig superfamily members reveals redundant and nonredundant roles for ICAM-1, ICAM-2, and VCAM-1 in lymphocyte homing. *Blood* 116(6):915–925.
17. Bajénoff M, et al. (2007) Highways, byways and breadcrumbs: Directing lymphocyte traffic in the lymph node. *Trends Immunol* 28(8):346–352.
18. Stein JV, Nombela-Arrieta C (2005) Chemokine control of lymphocyte trafficking: A general overview. *Immunology* 116(1):1–12.
19. Sobocinski GP, et al. (2010) Ultrastructural localization of extracellular matrix proteins of the lymph node cortex: Evidence supporting the reticular network as a pathway for lymphocyte migration. *BMC Immunol* 11:42.
20. Pouw NM, Westerlaken EJ, Willemsen RA, Debets R (2007) Gene transfer of human TCR in primary murine T cells is improved by pseudo-typing with amphotropic and ecotropic envelopes. *J Gene Med* 9(7):561–570.
21. Pan X, et al. (2012) HIV-1 Nef compensates for disorganization of the immunological synapse by inducing trans-Golgi network-associated Lck signaling. *Blood* 119(3): 786–797.
22. Volinsky N, Gantman A, Yablonski D (2006) A Pak- and Pix-dependent branch of the SDF-1alpha signalling pathway mediates T cell chemotaxis across restrictive barriers. *Biochem J* 397(1):213–222.
23. Faroudi M, et al. (2010) Critical roles for Rac GTPases in T-cell migration to and within lymph nodes. *Blood* 116(25):5536–5547.
24. Steiner O, et al. (2010) Differential roles for endothelial ICAM-1, ICAM-2, and VCAM-1 in shear-resistant T cell arrest, polarization, and directed crawling on blood-brain barrier endothelium. *J Immunol* 185(8):4846–4855.
25. Shulman Z, et al. (2012) Transendothelial migration of lymphocytes mediated by intraendothelial vesicle stores rather than by extracellular chemokine depots. *Nat Immunol* 13(1):67–76.
26. Alon R, Shulman Z (2011) Chemokine triggered integrin activation and actin remodeling events guiding lymphocyte migration across vascular barriers. *Exp Cell Res* 317(5):632–641.
27. Lämmermann T, et al. (2008) Rapid leukocyte migration by integrin-independent flowing and squeezing. *Nature* 453(7191):51–55.
28. Soriano SF, et al. (2011) In vivo analysis of uropod function during physiological T cell trafficking. *J Immunol* 187(5):2356–2364.
29. Murooka TT, et al. (2012) HIV-infected T cells are migratory vehicles for viral dissemination. *Nature* 490(7419):283–287.
30. Mukerji J, Olivieri KC, Misra V, Agopian KA, Gabuzda D (2012) Proteomic analysis of HIV-1 Nef cellular binding partners reveals a role for exocyst complex proteins in mediating enhancement of intercellular nanotube formation. *Retrovirology* 9:33.
31. Muller WA (2011) Mechanisms of leukocyte transendothelial migration. *Annu Rev Pathol* 6:323–344.
32. Cinamon G, Shinder V, Alon R (2001) Shear forces promote lymphocyte migration across vascular endothelium bearing apical chemokines. *Nat Immunol* 2(6):515–522.
33. Gérard A, van der Kammen RA, Janssen H, Ellenbroek SI, Collard JG (2009) The Rac activator Tiam1 controls efficient T-cell trafficking and route of transendothelial migration. *Blood* 113(24):6138–6147.
34. Heasman SJ, Carlin LM, Cox S, Ng T, Ridley AJ (2010) Coordinated RhoA signaling at the leading edge and uropod is required for T cell transendothelial migration. *J Cell Biol* 190(4):553–563.
35. Nombela-Arrieta C, et al. (2007) A central role for DOCK2 during interstitial lymphocyte motility and sphingosine-1-phosphate-mediated egress. *J Exp Med* 204(3): 497–510.
36. Shulman Z, et al. (2006) DOCK2 regulates chemokine-triggered lateral lymphocyte motility but not transendothelial migration. *Blood* 108(7):2150–2158.
37. Sánchez-Madrid F, del Pozo MA (1999) Leukocyte polarization in cell migration and immune interactions. *EMBO J* 18(3):501–511.
38. McMichael AJ, Borrow P, Tomaras GD, Goonetilleke N, Haynes BF (2010) The immune response during acute HIV-1 infection: Clues for vaccine development. *Nat Rev Immunol* 10(1):11–23.
39. Moir S, Fauci AS (2009) B cells in HIV infection and disease. *Nat Rev Immunol* 9(4): 235–245.
40. Muratori C, et al. (2009) Massive secretion by T cells is caused by HIV Nef in infected cells and by Nef transfer to bystander cells. *Cell Host Microbe* 6(3):218–230.
41. Stumptner-Cuvelette P, et al. (2001) HIV-1 Nef impairs MHC class II antigen presentation and surface expression. *Proc Natl Acad Sci USA* 98(21):12144–12149.
42. Swingler S, et al. (2008) Evidence for a pathogenic determinant in HIV-1 Nef involved in B cell dysfunction in HIV/AIDS. *Cell Host Microbe* 4(1):63–76.
43. Xu W, et al. (2009) HIV-1 evades virus-specific IgG2 and IgA responses by targeting systemic and intestinal B cells via long-range intercellular conduits. *Nat Immunol* 10 (9):1008–1017.
44. Fujii H, et al. (2011) HIV-1 Nef impairs multiple T-cell functions in antigen-specific immune response in mice. *Int Immunol* 23(7):433–441.
45. Sugimoto C, et al. (2003) nef gene is required for robust productive infection by simian immunodeficiency virus of T-cell-rich paracortex in lymph nodes. *J Virol* 77(7): 4169–4180.